

Capacitive PCB sensor for the detection of insects in intelligent traps

Leo Scherer
Sensorik-ApplikationsZentrum
OTH Regensburg
Ratisbon, Germany
leo.scherer@st.oth-regensburg.de

Thomas Vitzthumecker
Sensorik-ApplikationsZentrum
OTH Regensburg
Ratisbon, Germany
thomas.vitzthumecker@oth-regensburg.de

Rudolf Bierl
Sensorik-ApplikationsZentrum
OTH Regensburg
Ratisbon, Germany
rudolf.bierl@oth-regensburg.de

Abstract—Reliable and fast detection of pest in the food processing and pharmaceutical industry is crucial to ensure hygienically safe, pure and healthy products. This is why intelligent traps, that are able to detect insects automatically are needed. For this, a capacitive PCB sensor is developed and tested, which could be a simplistic, low power solution to the problem. This includes design, footprint generation and simulation as well as testing different types of capacitive sensing against noise immunity and sensitivity to *Blattella germanica*, the German cockroach. It is shown that a single specimen can very well and reliably be detected by the developed sensor.

I. INTRODUCTION

Reliable and fast detection of pest in the food processing and pharmaceutical industry is crucial to ensure hygienically safe, pure and healthy products that follow the “Hazard Analysis and Critical Control Point” principles [1].

A common solution to this problem are traps for pest monitoring, which need to be checked monthly by workers. This is a cumbersome and repetitive task which could be automated and simplified. This automation could provide constant, for example daily updated information on the current status of pest infection which leads to more precise counteractive measures with less pesticides and reduces the workload of the workers.

At a bigger scope, we try to develop a modular, universal remote pest sensing network, with battery powered sensor nodes build into traps that communicate over a low power wide area network and are build out of different modular components including a trap-type specific sensing unit, a power unit, a processing unit and a communication unit. They need to withstand the harsh industrial environments and should be long running and low cost.

Special focus lies on the development of the sensing unit, more precisely of a capacitive sensor array made out of capacitive sensing pads that are printed onto a printed circuit board (PCB). It aims to detect insects crossing over it or that are held in place by an adhesive surface.

Research concerning the capacitive detection of insects dates back to 1950. At this time, Backlund and Ekeroot presented their actograph, a machine build to record the movements of small terrestrial animals to better understand their daily cycle. It consisted of parallel, zig-zag-shaped copperwires, an oscillator and an amplifier and was able to detect the movement of blow flies, more precisely *Calliphora*

erythrocephala [2]. In the following years, this principle was iterated on multiple times, among others by Schechter et al. in 1963 for the recording of differences in the circadian rhythms of cockroaches on earth or in space [3], improved in sensitivity by Grobbelaar et al. in 1967 [4] or changed by Luff and Molyneux in 1970 to use operational amplifiers [5].

In the years after, it is hard to find other scientific works that explicitly use a capacitive detection method except for e.g. capacitive mosquito wing-beat sensors like presented in 2020 by Muralindran et al. [6]. Most current work focuses on detecting insects with camera based methods and nowadays machine learning. But capacitive sensors could provide a simplistic way with potentially lower power consumption and thus longer runtime.

This work concentrates on the design, development and testing of one of those capacitive sensing pads that should in the future build up a capacitive sensor array. First, a quick introduction to the theory of capacitive sensing is given. Then, the used methods are presented, including a footprint generator, simulation, production of the pads and the experimental setup for testing. Lastly, first experimental results are shown and a conclusion is given.

II. CAPACITIVE SENSING THEORY

Capacitive sensing describes the measurement of change in the capacitance between two sensing electrodes with different electric potentials. Between the two sensing electrodes, an electric field is formed. If this electric field or the relative permittivity of the medium is changed, the capacitance changes. This can be seen in Equation 1, where Q is the charge held on the sensing electrodes, V is the difference in electric potential, E is the electric field and ϵ the permittivity.

$$C = \frac{Q}{V} = \frac{\oint_A \epsilon_0 \cdot \epsilon_r \cdot \vec{E} \cdot d\vec{A}}{\int_S \vec{E} \cdot d\vec{s}} \quad (1)$$

A. Self and mutual capacitance sensing

When measuring capacitance of an conductor, either its self capacitance can be measured, which is the capacitance in respect to ground, or the mutual capacitance between two conductors can be measured.

In self capacitance sensing, only objects that are coupled to ground can be detected, as they increase the self capacitance of the sensor electrode (see Figure 1a). This is often used for presence or touch detection of humans, but does not work with small objects like insects.

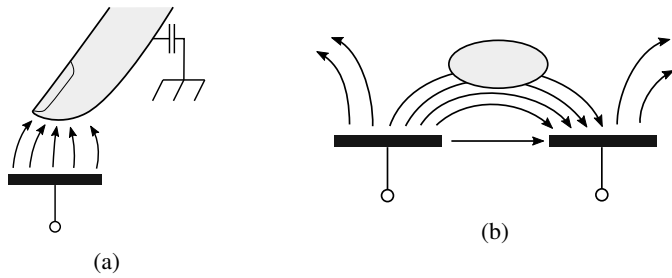


Figure 1: Self capacitance sensing (a) and mutual capacitance sensing (b) principle.

Mutual capacitance sensing measures the capacitance between two locally distinct sensing electrodes (see Figure 1b). Because of this the electrostatic field is well defined. Objects that are interacting with it or changing the relative permittivity of the medium are changing the capacitance. Therefore, also small objects can have an impact on the capacitance, if the relative permittivity of those objects is high enough to introduce a significant change in the electrostatic field. If none of the two sensing electrodes is grounded, it is called differential mutual capacitance sensing.

B. Challenges of small capacitances

The measured capacitances are in the order of multiple femtofarads. Even changes in cable spacing, length, and objects near it or in between the negative and positive sensing electrode have an impact on the measured capacitance. To shield the sensing cables against unwanted influence, a voltage-follower driven-shield can be used. This shield copies the potential of the sensing electrode, while being electrically disconnected. In contrast to a ground shield, there is no capacitive coupling between the shield and the sensing electrode as the potentials are equal. Therefore, no unwanted capacitance bias is introduced, which would reduce the sensitivity.

III. METHODS

As a specimen for testing the sensing pads, *Blattella germanica*, the German cockroach is used. It is placed on its feet in the middle of the pad with plastic tweezers. The specimen were frozen alive and only taken out for testing to keep them from drying out. As empirically tested, their capacitive influence is similar to living cockroaches. In previous works, it was shown that they can be reliably detected by an industrial capacitive distance sensor (Micro-Epsilon CS10) [7]. Because of this, its sensing principle was adapted to create the miniaturized PCB version. All PCB Layouts were done in KiCad EDA¹.

¹<https://www.kicad.org/>

A. Footprint Generator

To be able to create different and complex forms rapidly with an easy way of changing distances and parameters of the shape and form of the footprint, a footprint generator was developed and written in python. This footprint generator is based on KiCadModTree, a framework to create custom footprints². All footprints are generated using custom polygons, and self written drawing functions for the vertex placements, which allows for maximum customizability.

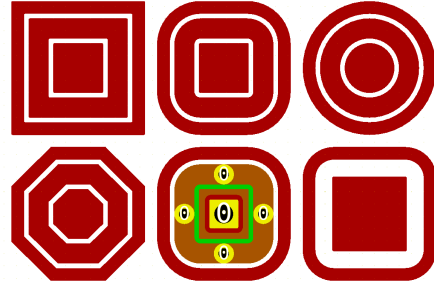


Figure 2: Different forms of footprints that are possible to generate with the developed footprint generator. The front layer of the PCB is colored in red, the back layer in green. Vias are yellow.

Some of the possible forms that currently can be created are displayed in Figure 2. The middle polygon always is the positive sensing electrode, the outer ring is the negative sensing electrode. The capacitance between those two is measured. If available, the middle ring is a voltage-follower driven shield (see Section II-B), or in this case also called a guard ring. It prohibits direct field lines between the sensing electrodes. In theory, this pushes the field lines out of the PCB plane into the air and should increase the sensitivity for changes above the sensing pad.

As can be seen in the top row, the rounding of the sensing pads can be customized as far as to get a perfect round circle. This parameter is useful to get a more homogeneous field distribution at the corners. All distances between the electrodes and their dimensions can be changed. By reducing the resolution of the edge rounding, octagonal shapes like the one at the bottom left can be generated. To test the influence of the guard ring, it can be left out. At last, as can be seen on the sensing pad in the middle of the bottom row, vias and backside shielding (guard backplate) can also be programatically placed.

The codebase can easily be adapted for other forms, such as hexagonal patterns. The generated footprint can be directly imported into KiCad.

B. Selected sensing pads

For testing, multiple pad types were generated, arranged on a 20 mm by 20 mm wide double-sided PCB and machined with a LPKF circuit board plotter. The tested variants are shown in Figure 3.

²<https://gitlab.com/kicad/libraries/kicad-footprint-generator>

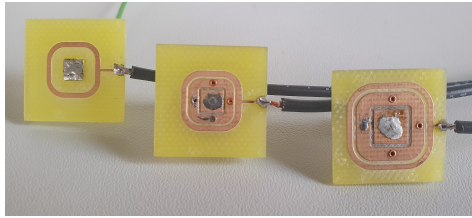


Figure 3: Selected variants of the sensing pad. The pad without guard ring is located on the left (pad 1), the shielded variant in the middle (pad 2) and a bigger one on the right (pad 3).

The standard sizes have a 4 mm by 4 mm wide positive sensing electrode with 0.1 mm inner radius, 0.4 mm spacing between the rings and a 1.6 mm thick guard ring with a guard backplate on the backside. The sensing pad on the right is scaled by a factor of 1.5, while the one on the left is without a guard ring. The variants with guard ring were tested with twisted pair cabling and later on fitted with a SMA connector on the backside to allow for coaxial cables. The shield of the coaxial cable is the same as the guard ring. The negative sensing electrode is connected on the right side on the front to reduce additional capacitance.

C. Simulation

Sensing pad design two from Figure 3 was simulated in Comsol Multiphysics³ with and without guard ring, with and without a guard backplate and also with and without a cockroach placed on top. This was done to get an idea of the influence of the cockroach on the measured capacitance and also to get an estimate for the absolute amount and resolution of capacitance that needs to be measured by the measurement circuit. The relative permittivity of the cockroach for the simulations was set to 2.7, as this is the relative permittivity of chitosan [8]. This can be considered a worst-case scenario, as the water content of a living specimen is between 68.4 % and 74.7 % and thus the real relative permittivity should be much higher [9].

D. Experimental set-up

The measurements were done at a temperature of 24.24 °C and a relative humidity of 41.12 %. The used measurement circuit is a ZSSC3230 Evaluation Kit, which features a Renesas ZSSC3230 IC for measuring capacitances in the pico- and femtofarad range. Only the raw values are recorded, which are not calibrated and therefore can not be used to get absolute capacitance values. The required power for the evaluation kit is provided through the USB-Port of a Laptop, which is plugged into the wall and consequently connected to earth ground. The data is transferred over USB and monitored live with an evaluation software provided by Renesas Electronics.

The ZSSC3230 features the possibility to measure self capacitance, mutual capacitance, mutual capacitance with a voltage-follower driven shield or differential mutual capacitance. Furthermore, a capacitance bias can be selected, which

gets subtracted from the measured values. Additionally, the capacitive measurement range can be selected from ± 0.5 pF to ± 16 pF. The ADC resolution can also be changed, with a maximum of 18 Bits and with an effective number of bits without oversampling of 14.4 due to noise. All capacitance values can be post-processed and temperature compensated internally [10].

For the measurements, all internal post-processing is turned off. The ADC resolution is set to 18 Bits and the measurement range to ± 0.5 pF. The bias capacitance as well as the measurement mode is adapted to the set-up.

There are 3 different experimental set-ups used to test the different sensing pads and connection methods. The sensing pad is always covered with a thin film of polyethylene to isolate the pad from the specimen.

Set-up one consists of sensing pad 1 which is connected in differential mutual capacitance measurement mode. As can be seen in Figure 4, the wires are spaced further apart, to reduce unwanted bias capacitance in the measurement.

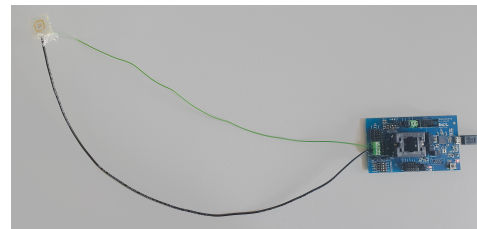


Figure 4: Experimental set-up one

In Figure 5 the second set-up is displayed. Sensing pad 3 is connected with a twisted pair cable, consisting of the sensing electrode and the driven shield, to the evaluation kit. The negative sensing electrode is connected to ground.

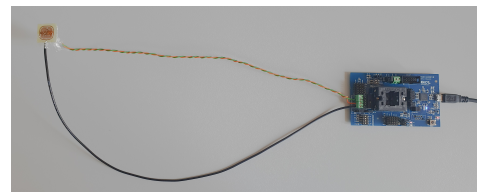


Figure 5: Experimental set-up two

In Figure 6 the third set-up is displayed. This set-up was tested with sensing pad 2 and sensing pad 3 fitted with a SMA connector. They are connected with a RG174 coaxial cable to reduce interference. The negative sensing electrode is connected to ground and twisted around the coaxial cable.

³<https://www.comsol.de/>

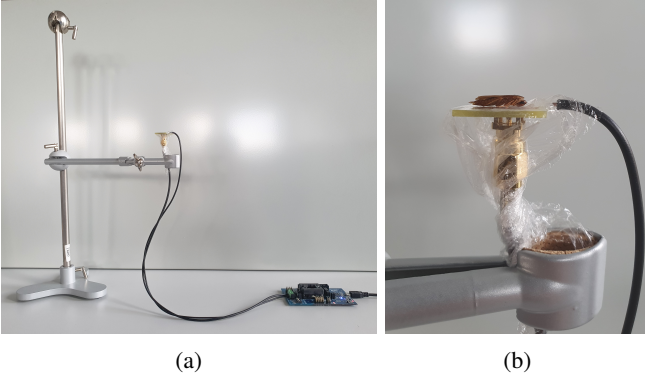


Figure 6: Experimental set-up three. Whole set-up (a) and close-up with added specimen, SMA connector and polyethylene insulation film (b).

IV. RESULTS

First, the results of the simulation are presented. Then, the experimental results are shown.

A. Simulation

The simulation results from Table I show capacitances in the femtofarad range, with absolute changes through the specimen ranging from 5.71 fF to 10.6 fF. As expected, the absolute capacitance of the sensing pad decreases with every step of additional shielding, as the driven shield is blocking the electrostatic field in unwanted areas. Furthermore, it forces the field out of the direct path and more to be above the sensing pad. Consequently, with added shielding the relative change in capacitance because of the added specimen increases.

| guard ring | guard backplate | specimen | capacitance [fF] | relative change [%] |
|------------|-----------------|----------|------------------|---------------------|
| ✓ | ✓ | | 14,91 | |
| ✓ | ✓ | ✓ | 20,62 | +38.3 |
| ✓ | | | 102,28 | |
| ✓ | | ✓ | 110,21 | +7.7 |
| | | | 300,17 | |
| | | ✓ | 310,77 | +3.5 |

Table I: Simulation results

B. Experimental set-up one

Figure 7a shows the measurement of capacitance where the cockroach is placed and removed two times on the sensing pad. Its influence can be seen by the two bumps in the graph. The absolute difference in raw sensor value, which is calculated by subtracting the two red averaging lines, is approx. 4000 units. With a full scale range of ± 0.5 pF, this translates to a change of approx. 15.3 fF (Equation 2).

Also visible is the relative high noise that is introduced by the relative long cables that act like an antenna. The influence of the cables and cable placement can be seen in Figure 7b where a hand is moved in and out of the area enclosed between the cables. Because of the missing shielding, both cables

form a capacitor between them. The hand interferes with the resulting electrostatic field and thus changes its capacitance.

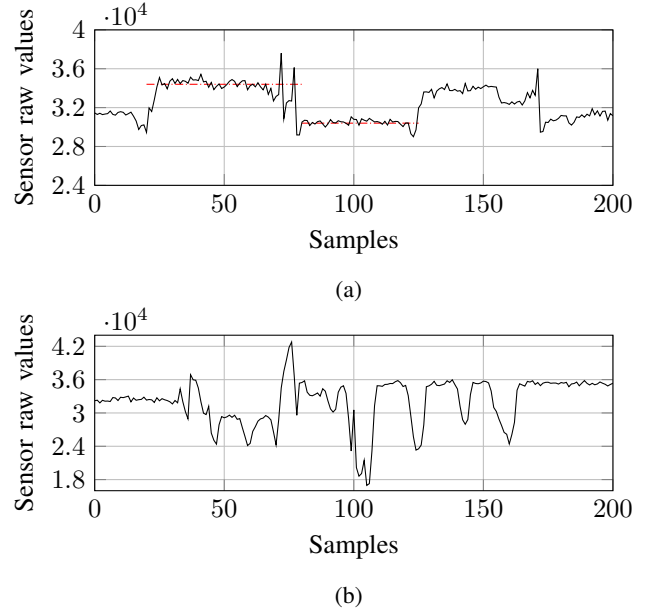


Figure 7: Results of experimental set-up one. Measured with a bias capacitance of 8.25 pF. Influence of cockroach on the sensing pad (a) with average lines drawn (red, dotted) and influence of hand movement between sensor cables (b).

$$\Delta C = \frac{1 \text{ pF}}{2^{18}} \cdot 4000 \approx 15.3 \text{ fF} \quad (2)$$

C. Experimental set-up two

With the addition of a guard ring and twisted pair cables, the noise floor is lower, as can be seen in Figure 8. The two bumps from the introduced specimen are clearly visible with an absolute difference of approx. 4800 units. This translates to a change of 18.3 fF. Also, hand movement near the cables did affect the measurements, but less than in the differential measurements.

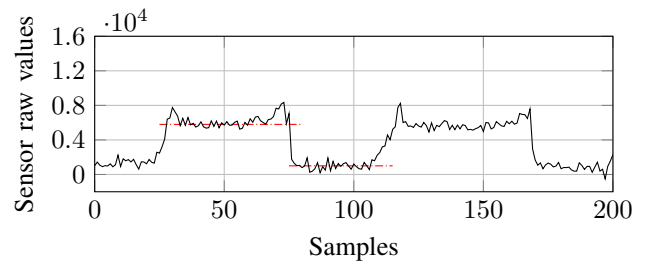


Figure 8: Results of experimental set-up two. Captured with a bias capacitance of 8.25 pF. Influence of cockroach on the sensing pad with average lines drawn (red, dotted).

D. Experimental set-up three

Replacing the twisted pair cable with a coaxial cable with SMA connector improved the noise and stability of the

measured signal significantly and blocked unwanted influence through nearby hand movement. Figure 9 shows the influence of the specimen placed again two times on the sensing pad. The first lower plateau in the graph is from a only halfway placed cockroach on the pad. As this got corrected, the measured capacitance rises to the second plateau, which it instantly reached when the cockroach is correctly placed the second time. The visible spikes at the start and end of the plateau come from the plastic tweezers that are used to place the specimen on the sensing pad.

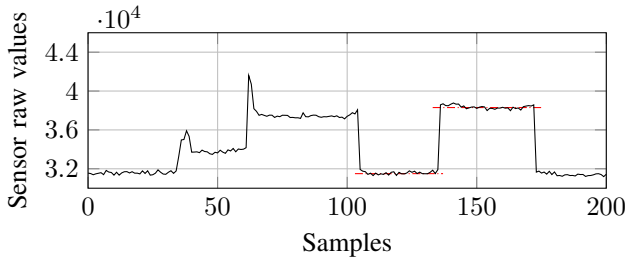


Figure 9: Results of experimental set-up three with sensing pad 2. Captured with a bias capacitance of 5.5 pF. Influence of cockroach on the sensing pad with average lines drawn (red, dotted).

The difference in raw sensor value is approx. 6800 units and therefore higher than in the other experiments. This translates to a change of 26 fF and is higher than expected.

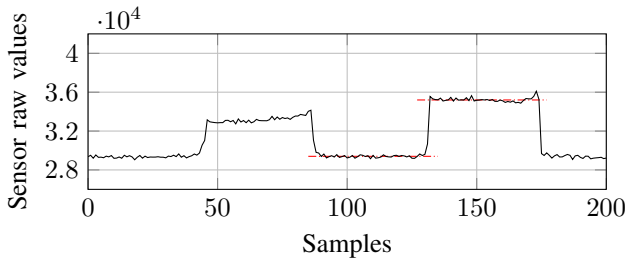


Figure 10: Results of experimental set-up three with the bigger sized sensing pad 3. Captured with a bias capacitance of 5.5 pF. Influence of cockroach on the sensing pad with average lines drawn (red, dotted).

When replaced by the bigger sized sensing pad, the sensitivity to further away objects increased subjectively. Additional measurements are necessary to scientifically prove this. As can be seen in Figure 10, the difference in raw sensor value is approx. 5800 units which equals to 22.1 fF.

V. CONCLUSION

As shown, one specimen is very well detectable by the developed capacitive PCB sensor and the used measurement circuit. Further measurements are needed, if the difference in raw sensor value should be compared between the different sensing pads and measurement modes, as the placement of the specimen on the pad was done by hand due to the lack of time and has a very significant impact. But, the sensor readings

are in the same order of magnitude as the simulations. Also, as the bigger sized sensing pad did not show an increase in sensitivity compared to the smaller sensing pad, the planed capacitive sensing array can be increased in resolution.

Several successful improvements were made to reduce noise and interference. In general, coaxial or even triaxial cables and a voltage-follower driven shield should be used whenever possible. Twisted pair cables are not sufficient to effectively shield the sensing electrode.

In the future, the sensing pads and different possible shapes need to be further analyzed to find the optimal sensing pad design. For this task, the developed footprint generator helps with rapid testing.

REFERENCES

- [1] European Parliament and Council, Regulation (EC) No 852/2004, "on the hygiene of foodstuffs," 2004.
- [2] H. O. Backlund and S. Ekeroot, "An Actograph for Small Terrestrial Animals," *Oikos*, vol. 2, no. 2, pp. 213–216, 1950.
- [3] M. S. Schechter, S. R. Dutky, and W. N. Sullivan, "Recording Circadian Rhythms of the Cockroach with a Capacity-Sensing Device," *Journal of Economic Entomology*, vol. 56, no. 1, pp. 76–79, Feb. 1963.
- [4] J. H. Grobbelaar, G. J. Morrison, E. E. Baart, and V. C. Moran, "A versatile, highly sensitive activity recorder for insects," *Journal of Insect Physiology*, vol. 13, no. 12, pp. 1843–1848, Dec. 1967.
- [5] M. L. Luff and L. Molyneux, "Insect movement detector using operational amplifiers," *Journal of Physics E: Scientific Instruments*, vol. 3, no. 11, pp. 939–941, Nov. 1970.
- [6] M. Muralindran, R. P. Rosalyn, W. W. Kitt, and T. T. Brendan Khoo, "Capacitive Mosquito Wing-beat Sensor: A Novel Sensor for Intelligent Traps," *IJERA Journal*, vol. 10, no. 7, pp. 18–27, Aug. 2020.
- [7] L. Scherer, "Evaluation of capacitive sensing for pest detection and monitoring," Jan. 2021.
- [8] C. Lima, R. de Oliveira, S. Figueiró, C. Wehmann, J. Góes, and A. Sombra, "Dc conductivity and dielectric permittivity of collagen–chitosan films," *Materials Chemistry and Physics*, vol. 99, no. 2, pp. 284–288, 2006.
- [9] A. Appel and M. Tanley, "Water composition and loss by body color and form mutants of the German cockroach (Dictyoptera: Blattellidae)," *Comparative Biochemistry and Physiology Part A: Molecular & Integrative Physiology*, vol. 122, no. 4, pp. 415–420, 1999.
- [10] Renesas Electronics Corporation, "ZSSC3230 datasheet," Oct. 2019.